



# A Data Driven Toggling Gain Complementary Filtering Approach for Orientation Estimation

**Network and Data Analysis Group**

Samnun Azfar - 200041130

Ramisa Zaman Audhi - 200041131

Mir Md Inzamam - 200041240

**Supervised by**

Abu Raihan Mostofa Kamal

Professor

Department of CSE

Islamic University of Technology

**Co-supervised by**

Mohammad Ishrak Abedin

Lecturer

Department of CSE

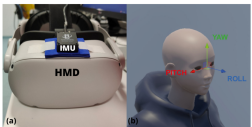
Islamic University of Technology

# **Introduction**

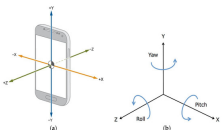
---

# Applications of Orientation Algorithms and IMUs

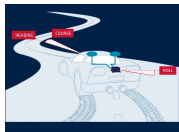
## Real World Applications



VR Head-mount



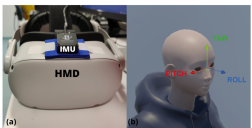
Smartphone orientation



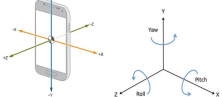
Autonomous vehicles

# Applications of Orientation Algorithms and IMUs

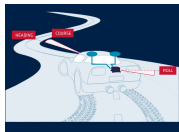
## Real World Applications



VR Head-mount



Smartphone orientation



Autonomous vehicles

## IMU and MARG Sensors



IMU and MARG sensors applications

# Sensor Fusion Concept

---

- Individual sensors have complementary strengths: - **gyroscopes** measure rotation but **drift over time**, **accelerometers** measure tilt via gravity but are **noisy during movement**, **magnetometers** give heading but are **disturbed by local fields**.

# Sensor Fusion Concept

---

- Individual sensors have complementary strengths: - **gyroscopes** measure rotation but **drift over time**, **accelerometers** measure tilt via gravity but are **noisy during movement**, **magnetometers** give heading but are **disturbed by local fields**.
- Sensor fusion algorithms (e.g., Kalman[15][7][16] or complementary filters[11]) combine these readings to obtain a stable orientation estimate. By using multiple sensors, we can “**reduce orientation drift introduced through the gyroscope measurements**” using gravity and magnetic references.

# Sensor Fusion Concept

---

- Individual sensors have complementary strengths: - **gyroscopes** measure rotation but **drift over time**, **accelerometers** measure tilt via gravity but are **noisy during movement**, **magnetometers** give heading but are **disturbed by local fields**.
- Sensor fusion algorithms (e.g., Kalman[15][7][16] or complementary filters[11]) combine these readings to obtain a stable orientation estimate. By using multiple sensors, we can **“reduce orientation drift introduced through the gyroscope measurements”** using gravity and magnetic references.

## Goal

The goal is to filter out noise and biases: high-frequency noise from accelerometers is smoothed, while low-frequency gyro drift is corrected by accelerometer/magnetometer data, yielding a robust attitude estimate.

# Complementary Filter (CF) Overview

---

## General Equation of the Weighted Sum

$$\theta(t) = (1 - \alpha) \text{ (gyro-integrated angle)} + \alpha \text{ (accel-derived angle)}$$

- The blending weight  $\alpha$  (between 0 and 1) is tuned based on sensor characteristics.

# Complementary Filter (CF) Overview

## General Equation of the Weighted Sum

$$\theta(t) = (1 - \alpha) (\text{gyro-integrated angle}) + \alpha (\text{accel-derived angle})$$

- The blending weight  $\alpha$  (between 0 and 1) is tuned based on sensor characteristics.

## Advantages

- Very simple and efficient to implement on microcontrollers.
- Requires minimal computation.
- Reduces random noise (accelerometer) and drift (gyroscope)[18].

# Complementary Filter (CF) Overview

## General Equation of the Weighted Sum

$$\theta(t) = (1 - \alpha) \text{ (gyro-integrated angle)} + \alpha \text{ (accel-derived angle)}$$

- The blending weight  $\alpha$  (between 0 and 1) is tuned based on sensor characteristics.

### Advantages

- Very simple and efficient to implement on microcontrollers.
- Requires minimal computation.
- Reduces random noise (accelerometer) and drift (gyroscope)[18].

### Disadvantages

- Fixed filter gains cannot adapt to changing dynamics or sensor conditions.
- Gyroscope biases over time introduce drift if not perfectly zeroed.
- Assumes a stable magnetic reference—disturbances cause yaw drift.

## **Uses and Applications**

---

# Consequences of Poor Orientation Estimation

---

- In **VR/AR**, **incorrect orientation** causes virtual objects to **lag or shift unexpectedly**, leading to **user disorientation or motion sickness**. The “reality” no longer matches the user’s motions.

# Consequences of Poor Orientation Estimation

---

- In **VR/AR**, **incorrect orientation** causes virtual objects to **lag or shift unexpectedly**, leading to **user disorientation or motion sickness**. The “reality” no longer matches the user’s motions.
- In **navigation (drones, aircraft, robotics)**, **bad attitude estimates** can cause **control errors or crashes**. For example, a drone in strong magnetic interference may misread its yaw and slowly rotate off course.

# Consequences of Poor Orientation Estimation

---

- In **VR/AR**, **incorrect orientation** causes virtual objects to **lag or shift unexpectedly**, leading to **user disorientation or motion sickness**. The “reality” no longer matches the user’s motions.
- In **navigation (drones, aircraft, robotics)**, **bad attitude estimates** can cause **control errors or crashes**. For example, a drone in strong magnetic interference may misread its yaw and slowly rotate off course.
- **Inertial systems** are immune to jamming (no external signals needed), but they rely on **sensor accuracy**. If magnetic disturbances occur, a MARG system “**will over time result in a drift in the heading estimate**”.

## **Literature Review**

---

# Literature Review (Paper 1)

---

## Adaptive Attitude Estimation Using a Hybrid Model-Learning Approach (2022) [19]

**Authors:** Eran Vertzberger, Itzik Klein

**Journal:** IEEE Transactions on Instrumentation and Measurement

### Overview:

Demonstrates a **hybrid adaptive complementary filter** that learns axis-specific accelerometer weights via neural networks. Quaternion gyro data is integrated and a complementary update is applied in each axis whose weight is predicted by a small neural network based on estimated linear accelerations.

### Evaluation:

- Smartphone IMU dataset (60 two-minute sequences of walking activities in pocket, hand, etc., with VI-SLAM ground truth)

### Benchmark:

- Fixed-gain filters (Mahony[14], Madgwick[13])

### Contributions:

- Learned filter (DAE) yielded the lowest roll/pitch errors (10–37% better than classic filters).
- Adapts to dynamic motion via data-driven weight tuning.
- Outperforms fixed gains under varying conditions.

### Disadvantages:

- Requires labeled training data and offline learning.
- Neural nets add complexity.
- Yaw is not addressed (no magnetometer fusion).

# Literature Review (Paper 2)

---

## A Robust Complementary Filter Approach for Attitude Estimation of Unmanned Aerial Vehicles using AHRS (2019) [1]

**Authors:** Johann Meyer, Kreelan Padayachee, Benjamin A. Broughton

**Conference:** CEAS EuroGNC 2019

### Overview:

Explicitly detects when accelerometers are unreliable based on “steadiness” measure (using a low-pass on the accel magnitude) to decide if the vehicle is in steady flight. When unsteady, the filter relies on gyro propagation only; when steady, normal fusion occurs. A Gaussian random-walk model for gyro bias is implemented that rejects improbable bias drifts during maneuvers. **Evaluation:**

- Monte Carlo simulations (maneuvering UAV trajectories)

### Contributions:

- Monte Carlo simulations show their filter tracks roll dynamics more accurately than standard CFs[11].
- Simple gating logic avoids gross errors from accelerometer disturbances.
- Robust gyro bias handling.

### Disadvantages:

- Effectively disables accelerometer fusion during dynamics (so short-term drift may grow).
- Requires tuning of “steadiness” thresholds.
- Only tested in simulations.

# Literature Review (Paper 3)

---

## Denoising IMU Gyroscopes With Deep Learning for Open-Loop Attitude Estimation (2020)

[4]

**Authors:** Martin Brossard, Silvère Bonnabel, Axel Barrau

**Journal:** IEEE Robotics and Automation Letters (Volume: 5, Issue: 3, July 2020)

### Overview:

A deep convolutional network to denoise IMU gyroscopes for open-loop attitude estimation is introduced, where a CNN (with dilated convolutions) is trained on ground-truth data so that it outputs corrected gyro increments. The orientation is then obtained by simply integrating these denoised increments in dead-reckoning. Their loss is carefully designed for angular increments, and no RNNs are used (making inference fast).

### Evaluation:

- EuRoC and TUM-VI Datasets

### Contributions:

- Outperforms state-of-the-art methods and even beats top visual-inertial odometry algorithms in attitude accuracy.
- End-to-end learned correction captures complex noise/scale drift.
- No vision needed yet achieves very low drift.

### Disadvantages:

- Requires large ground-truth datasets for training design is more complex.
- Open-loop mode still drifts (albeit slower).
- Network complexity.

# Gaps and Opportunities

Problems	Solutions
<p><b>Lack of Real-Time Adaptivity:</b></p> <ul style="list-style-type: none"><li>• Static parameters cannot adapt to dynamic changes [9], [11], [13]</li><li>• Unexpected accelerations degrade accuracy [10]</li></ul>	<p><b>Adaptive Learning:</b></p> <ul style="list-style-type: none"><li>• Dual-XGBoost adjusts fusion weights online</li><li>• Responds dynamically to abrupt motions/disturbances</li></ul>

# Gaps and Opportunities

Problems	Solutions
<b>Lack of Real-Time Adaptivity:</b> <ul style="list-style-type: none"><li>• Static parameters cannot adapt to dynamic changes [9], [11], [13]</li><li>• Unexpected accelerations degrade accuracy [10]</li></ul>	<b>Adaptive Learning:</b> <ul style="list-style-type: none"><li>• Dual-XGBoost adjusts fusion weights online</li><li>• Responds dynamically to abrupt motions/disturbances</li></ul>
<b>Lack of Explicit Noise Prediction:</b> <ul style="list-style-type: none"><li>• EKFs assume constant noise, can't predict drift [7], [15], [16]</li><li>• Fail under temperature/vibration-induced noise [8]</li></ul>	<b>Predictive Noise Modeling:</b> <ul style="list-style-type: none"><li>• XGBoost predicts gyro bias/variance in real-time</li><li>• Learns time-varying noise for accuracy</li></ul>

# Gaps and Opportunities

Problems	Solutions
<b>Lack of Real-Time Adaptivity:</b> <ul style="list-style-type: none"><li>• Static parameters cannot adapt to dynamic changes [9], [11], [13]</li><li>• Unexpected accelerations degrade accuracy [10]</li></ul>	<b>Adaptive Learning:</b> <ul style="list-style-type: none"><li>• Dual-XGBoost adjusts fusion weights online</li><li>• Responds dynamically to abrupt motions/disturbances</li></ul>
<b>Lack of Explicit Noise Prediction:</b> <ul style="list-style-type: none"><li>• EKFs assume constant noise, can't predict drift [7], [15], [16]</li><li>• Fail under temperature/vibration-induced noise [8]</li></ul>	<b>Predictive Noise Modeling:</b> <ul style="list-style-type: none"><li>• XGBoost predicts gyro bias/variance in real-time</li><li>• Learns time-varying noise for accuracy</li></ul>
<b>Over-Reliance on Fixed Gains:</b> <ul style="list-style-type: none"><li>• Fixed gains cause large errors in dynamic motions [10], [13]</li><li>• Hard to balance under- vs over-correction [15], [17]</li></ul>	<b>Dynamic Gain Tuning:</b> <ul style="list-style-type: none"><li>• XGBoost adaptively infers fusion weights</li><li>• Removes need for manual tuning</li></ul>

# Gaps and Opportunities

Problems	Solutions
<b>Lack of Real-Time Adaptivity:</b> <ul style="list-style-type: none"><li>• Static parameters cannot adapt to dynamic changes [9], [11], [13]</li><li>• Unexpected accelerations degrade accuracy [10]</li></ul>	<b>Adaptive Learning:</b> <ul style="list-style-type: none"><li>• Dual-XGBoost adjusts fusion weights online</li><li>• Responds dynamically to abrupt motions/disturbances</li></ul>
<b>Lack of Explicit Noise Prediction:</b> <ul style="list-style-type: none"><li>• EKFs assume constant noise, can't predict drift [7], [15], [16]</li><li>• Fail under temperature/vibration-induced noise [8]</li></ul>	<b>Predictive Noise Modeling:</b> <ul style="list-style-type: none"><li>• XGBoost predicts gyro bias/variance in real-time</li><li>• Learns time-varying noise for accuracy</li></ul>
<b>Over-Reliance on Fixed Gains:</b> <ul style="list-style-type: none"><li>• Fixed gains cause large errors in dynamic motions [10], [13]</li><li>• Hard to balance under- vs over-correction [15], [17]</li></ul>	<b>Dynamic Gain Tuning:</b> <ul style="list-style-type: none"><li>• XGBoost adaptively infers fusion weights</li><li>• Removes need for manual tuning</li></ul>
<b>Heavy Computational Burden:</b> <ul style="list-style-type: none"><li>• DNNs and advanced EKFs too heavy for real-time [1], [2], [4]</li><li>• Require GPUs or powerful processors [6]</li></ul>	<b>Lightweight Inference:</b> <ul style="list-style-type: none"><li>• XGBoost is runtime efficient</li><li>• Suitable for micro-controllers</li></ul>

# Gaps and Opportunities

Problems	Solutions
<b>Lack of Real-Time Adaptivity:</b> <ul style="list-style-type: none"><li>• Static parameters cannot adapt to dynamic changes [9], [11], [13]</li><li>• Unexpected accelerations degrade accuracy [10]</li></ul>	<b>Adaptive Learning:</b> <ul style="list-style-type: none"><li>• Dual-XGBoost adjusts fusion weights online</li><li>• Responds dynamically to abrupt motions/disturbances</li></ul>
<b>Lack of Explicit Noise Prediction:</b> <ul style="list-style-type: none"><li>• EKFs assume constant noise, can't predict drift [7], [15], [16]</li><li>• Fail under temperature/vibration-induced noise [8]</li></ul>	<b>Predictive Noise Modeling:</b> <ul style="list-style-type: none"><li>• XGBoost predicts gyro bias/variance in real-time</li><li>• Learns time-varying noise for accuracy</li></ul>
<b>Over-Reliance on Fixed Gains:</b> <ul style="list-style-type: none"><li>• Fixed gains cause large errors in dynamic motions [10], [13]</li><li>• Hard to balance under- vs over-correction [15], [17]</li></ul>	<b>Dynamic Gain Tuning:</b> <ul style="list-style-type: none"><li>• XGBoost adaptively infers fusion weights</li><li>• Removes need for manual tuning</li></ul>
<b>Heavy Computational Burden:</b> <ul style="list-style-type: none"><li>• DNNs and advanced EKFs too heavy for real-time [1], [2], [4]</li><li>• Require GPUs or powerful processors [6]</li></ul>	<b>Lightweight Inference:</b> <ul style="list-style-type: none"><li>• XGBoost is runtime efficient</li><li>• Suitable for micro-controllers</li></ul>
<b>Loss of Interpretability:</b> <ul style="list-style-type: none"><li>• Deep models act as black-box [1], [2], [4]</li><li>• Lack of physical insight complicates debugging [6]</li></ul>	<b>Transparent Design:</b> <ul style="list-style-type: none"><li>• XGBoost trees are interpretable</li><li>• Fusion logic tied explicitly to physics</li></ul>

# Our Contribution

---

- **$\alpha$ -Toggling Based on Data-Driven Movement Prediction** For deciding when to fuse accelerometer and when to rely on gyroscope readings alone.

# Our Contribution

---

- **$\alpha$ -Toggling Based on Data-Driven Movement Prediction** For deciding when to fuse accelerometer and when to rely on gyroscope readings alone.
- **Denoising Based on Tree-Based Model:** Predicting the noise and filtering it out of the raw readings before computation.

# Our Contribution

---

- **$\alpha$ -Toggling Based on Data-Driven Movement Prediction** For deciding when to fuse accelerometer and when to rely on gyroscope readings alone.
- **Denoising Based on Tree-Based Model:** Predicting the noise and filtering it out of the raw readings before computation.
- **Construction of a Mechanical Turntable for Real-Life Evaluation:** For evaluating the validity of our model based on real-life movement and scenarios.

## **Proposed Solution**

---

# Proposed Modified Complementary Filter

---

## Noise Prediction & Removal [4]

- Input raw sensor (acc, mag, gyro) columns:  
 $a_i = (a_{ix}, a_{iy}, a_{iz})$ ,  $m_i = (m_{ix}, m_{iy}, m_{iz})$ ,  
 $g_i = (g_{ix}, g_{iy}, g_{iz})$ .

# Proposed Modified Complementary Filter

---

## Noise Prediction & Removal [4]

- Input raw sensor (acc, mag, gyro) columns:  
 $a_i = (a_{ix}, a_{iy}, a_{iz})$ ,  $m_i = (m_{ix}, m_{iy}, m_{iz})$ ,  
 $g_i = (g_{ix}, g_{iy}, g_{iz})$ .
- Trained regressor predicts noise components  
 $\eta_a, \eta_m$ .

# Proposed Modified Complementary Filter

---

## Noise Prediction & Removal [4]

- Input raw sensor (acc, mag, gyro) columns:  
 $a_i = (a_{ix}, a_{iy}, a_{iz})$ ,  $m_i = (m_{ix}, m_{iy}, m_{iz})$ ,  
 $g_i = (g_{ix}, g_{iy}, g_{iz})$ .
- Trained regressor predicts noise components  
 $\eta_a, \eta_m$ .
- Denoised vectors:

$$a_i = a_i - \eta_a, \quad m_i = m_i - \eta_m$$

$$a_{pred} = R_g * a_{(i-1)pred} (1 - \alpha) + \alpha * a_i$$

$$m_{pred} = R_g * m_{(i-1)pred} (1 - \alpha) + \alpha * m_i$$

# Proposed Modified Complementary Filter

---

## Noise Prediction & Removal [4]

- Input raw sensor (acc, mag, gyro) columns:  
 $a_i = (a_{ix}, a_{iy}, a_{iz})$ ,  $m_i = (m_{ix}, m_{iy}, m_{iz})$ ,  
 $g_i = (g_{ix}, g_{iy}, g_{iz})$ .
- Trained regressor predicts noise components  
 $\eta_a, \eta_m$ .
- Denoised vectors:

$$a_i = a_i - \eta_a, \quad m_i = m_i - \eta_m$$

$$a_{pred} = R_g * a_{(i-1)pred}(1 - \alpha) + \alpha * a_i$$

$$m_{pred} = R_g * m_{(i-1)pred}(1 - \alpha) + \alpha * m_i$$

- In the above equations  $R_g$  is the quaternion or rotation matrix [3][5].

# Proposed Modified Complementary Filter

## Noise Prediction & Removal [4]

- Input raw sensor (acc, mag, gyro) columns:  
 $a_i = (a_{ix}, a_{iy}, a_{iz})$ ,  $m_i = (m_{ix}, m_{iy}, m_{iz})$ ,  
 $g_i = (g_{ix}, g_{iy}, g_{iz})$ .
- Trained regressor predicts noise components  
 $\eta_a, \eta_m$ .
- Denoised vectors:

$$a_i = a_i - \eta_a, \quad m_i = m_i - \eta_m$$

$$a_{pred} = R_g * a_{(i-1)pred}(1 - \alpha) + \alpha * a_i$$

$$m_{pred} = R_g * m_{(i-1)pred}(1 - \alpha) + \alpha * m_i$$

- In the above equations  $R_g$  is the quaternion or rotation matrix [3][5].

## Movement Prediction & $\alpha$ Toggling [19]

- Toggling Engine analyzes  $g_i$  (gyro) patterns to classify motion state.

# Proposed Modified Complementary Filter

## Noise Prediction & Removal [4]

- Input raw sensor (acc, mag, gyro) columns:  
 $a_i = (a_{ix}, a_{iy}, a_{iz})$ ,  $m_i = (m_{ix}, m_{iy}, m_{iz})$ ,  
 $g_i = (g_{ix}, g_{iy}, g_{iz})$ .
- Trained regressor predicts noise components  
 $\eta_a, \eta_m$ .
- Denoised vectors:

$$a_i = a_i - \eta_a, \quad m_i = m_i - \eta_m$$

$$a_{pred} = R_g * a_{(i-1)pred}(1 - \alpha) + \alpha * a_i$$

$$m_{pred} = R_g * m_{(i-1)pred}(1 - \alpha) + \alpha * m_i$$

- In the above equations  $R_g$  is the quaternion or rotation matrix [3][5].

## Movement Prediction & $\alpha$ Toggling [19]

- Toggling Engine analyzes  $g_i$  (gyro) patterns to classify motion state.
- Generates adaptive gain  $\alpha$  based on predicted movement (static vs. dynamic).

# Proposed Modified Complementary Filter

## Noise Prediction & Removal [4]

- Input raw sensor (acc, mag, gyro) columns:  
 $a_i = (a_{ix}, a_{iy}, a_{iz})$ ,  $m_i = (m_{ix}, m_{iy}, m_{iz})$ ,  
 $g_i = (g_{ix}, g_{iy}, g_{iz})$ .
- Trained regressor predicts noise components  
 $\eta_a, \eta_m$ .
- Denoised vectors:

$$a_i = a_i - \eta_a, \quad m_i = m_i - \eta_m$$

$$a_{pred} = R_g * a_{(i-1)pred}(1 - \alpha) + \alpha * a_i$$

$$m_{pred} = R_g * m_{(i-1)pred}(1 - \alpha) + \alpha * m_i$$

- In the above equations  $R_g$  is the quaternion or rotation matrix [3][5].

## Movement Prediction & $\alpha$ Toggling [19]

- Toggling Engine analyzes  $g_i$  (gyro) patterns to classify motion state.
- Generates adaptive gain  $\alpha$  based on predicted movement (static vs. dynamic).
- Compute gyro-based update:

$$R_g = \exp\left(\Omega_{\times}(g_i) \delta t\right)$$

where  $\Omega_{\times}$  is the skew-symmetric operator [20].

# Proposed Modified Complementary Filter

## Noise Prediction & Removal [4]

- Input raw sensor (acc, mag, gyro) columns:  
 $a_i = (a_{ix}, a_{iy}, a_{iz})$ ,  $m_i = (m_{ix}, m_{iy}, m_{iz})$ ,  
 $g_i = (g_{ix}, g_{iy}, g_{iz})$ .
- Trained regressor predicts noise components  
 $\eta_a, \eta_m$ .
- Denoised vectors:

$$a_i = a_i - \eta_a, \quad m_i = m_i - \eta_m$$

$$a_{pred} = R_g * a_{(i-1)pred}(1 - \alpha) + \alpha * a_i$$

$$m_{pred} = R_g * m_{(i-1)pred}(1 - \alpha) + \alpha * m_i$$

- In the above equations  $R_g$  is the quaternion or rotation matrix [3][5].

## Movement Prediction & $\alpha$ Toggling [19]

- Toggling Engine analyzes  $g_i$  (gyro) patterns to classify motion state.
- Generates adaptive gain  $\alpha$  based on predicted movement (static vs. dynamic).
- Compute gyro-based update:

$$R_g = \exp\left(\Omega_{\times}(g_i) \delta t\right)$$

where  $\Omega_{\times}$  is the skew-symmetric operator [20].

- Final CF fusion in 1:

$$R = (1 - \alpha) R_g + \alpha R_{am}.$$

# Proposed Modified Complementary Filter

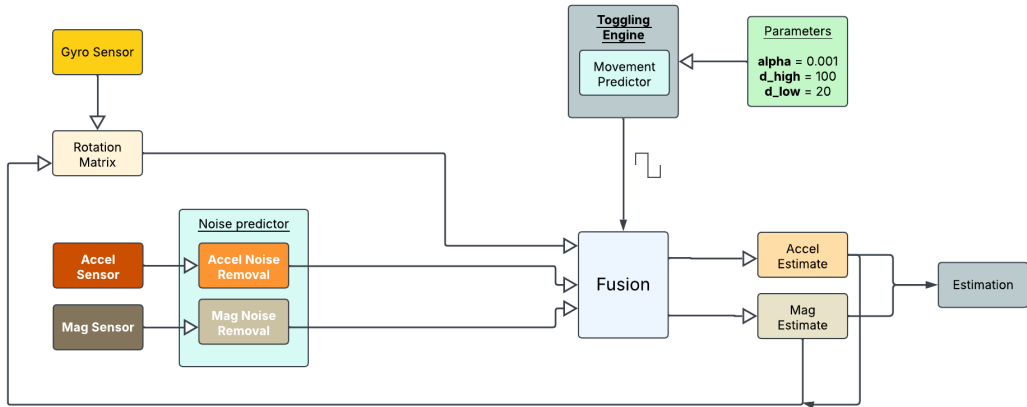


Figure: Toggling Engine: Modified Filter Diagram with Noise Prediction and Movement Prediction

# Dataset Overview: BROAD

---

- Berlin Robust Orientation Estimation Assessment Dataset (BROAD) [12]

## Dataset Overview: BROAD

---

- Berlin Robust Orientation Estimation Assessment Dataset (BROAD) [12]
- Trials: 39 recordings of predefined motions

# Dataset Overview: BROAD

---

- Berlin Robust Orientation Estimation Assessment Dataset (BROAD) [12]
- **Trials:** 39 recordings of predefined motions
- **Sampling:**
  - OptiTrack ground truth: position opt\_pos & orientation opt\_quat at 120Hz
  - IMU MARG data: accelerometer, gyroscope, magnetometer at 286Hz
  - Boolean movement flag per timestamp

# Dataset Overview: BROAD

---

- Berlin Robust Orientation Estimation Assessment Dataset (BROAD) [12]
- **Trials:** 39 recordings of predefined motions
- **Sampling:**
  - OptiTrack ground truth: position opt\_pos & orientation opt\_quat at 120Hz
  - IMU MARG data: accelerometer, gyroscope, magnetometer at 286Hz
  - Boolean movement flag per timestamp
- **Hardware:**
  - Custom 3D-printed mount with myon aktos-t 9-axis IMU
  - Optical markers for tracking by OptiTrack OMC system

# Dataset Overview: BROAD

---

- Berlin Robust Orientation Estimation Assessment Dataset (BROAD) [12]
- **Trials:** 39 recordings of predefined motions
- **Sampling:**
  - OptiTrack ground truth: position opt\_pos & orientation opt\_quat at 120Hz
  - IMU MARG data: accelerometer, gyroscope, magnetometer at 286Hz
  - Boolean movement flag per timestamp
- **Hardware:**
  - Custom 3D-printed mount with myon aktos-t 9-axis IMU
  - Optical markers for tracking by OptiTrack OMC system
- **Motion types:** undisturbed (rotation, translation, combined; slow/fast) and disturbed (tapping, vibration, magnets, office, mixed)

# Dataset Overview: BROAD

---

- Berlin Robust Orientation Estimation Assessment Dataset (BROAD) [12]
- **Trials:** 39 recordings of predefined motions
- **Sampling:**
  - OptiTrack ground truth: position opt\_pos & orientation opt\_quat at 120Hz
  - IMU MARG data: accelerometer, gyroscope, magnetometer at 286Hz
  - Boolean movement flag per timestamp
- **Hardware:**
  - Custom 3D-printed mount with myon aktos-t 9-axis IMU
  - Optical markers for tracking by OptiTrack OMC system
- **Motion types:** undisturbed (rotation, translation, combined; slow/fast) and disturbed (tapping, vibration, magnets, office, mixed)
- Detailed protocol in the BROAD paper:  
<https://www.mdpi.com/2306-5729/6/7/72>

# Dataset Snapshot

---

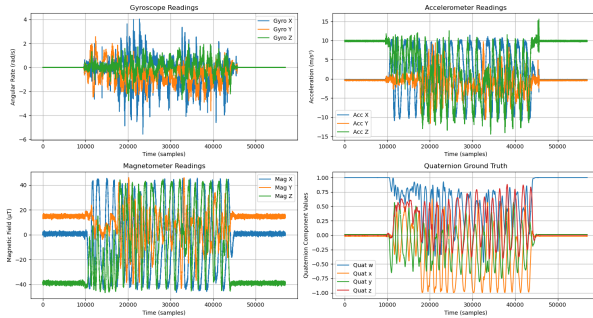


Figure: Snapshot of the recording of the file "01\_undisturbed\_low\_rotation\_A"

# Dataset Details: Categories & Hardware

---

Motion Type	Speed	Indices
<b>Undisturbed</b>		
Rotation	Slow	01–05
Rotation	Fast	06–09
Translation	Slow	10–14
Translation	Fast	15–18
Combined	Slow	19–20
Combined	Fast	21–23
<b>Disturbed (Medium Speed)</b>		
Tapping	—	24–25
Vibrating Smart-phone	—	26–27
Stationary Magnet	—	28–31
Attached Magnet (1–5)	—	32–36
Office Environment	—	37–38
Mixed	—	39

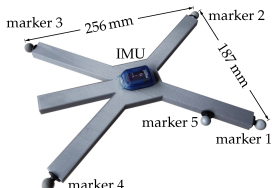
# Dataset Details: Categories & Hardware

Motion Type	Speed	Indices
<b>Undisturbed</b>		
Rotation	Slow	01–05
Rotation	Fast	06–09
Translation	Slow	10–14
Translation	Fast	15–18
Combined	Slow	19–20
Combined	Fast	21–23
<b>Disturbed (Medium Speed)</b>		
Tapping	—	24–25
Vibrating Smart-phone	—	26–27
Stationary Magnet	—	28–31
Attached Magnet (1–5)	—	32–36
Office Environment	—	37–38
Mixed	—	39

01\_undisturbed\_slow\_rotation\_A.hdf5

- imu\_acc
- imu\_gyr
- imu\_mag
- movement
- opt\_pos
- opt\_quat

(a) Dataset columns overview



(b) 3D-printed mount with IMU (OptiTrack markers)

## **Experimental Setup**

---

# Training to Predict Movement Noise: Dataset

---

- **Movement Prediction Model:** Train **XGB classifier** to predict if the IMU is in motion.

# Training to Predict Movement Noise: Dataset

---

- **Movement Prediction Model:** Train **XGB classifier** to predict if the IMU is in motion.
- **Noise Prediction Model:** Train **XGB regressor** to predict noises in raw accelerometer data.

# Training to Predict Movement Noise: Dataset

---

- **Movement Prediction Model:** Train **XGB classifier** to predict if the IMU is in motion.
- **Noise Prediction Model:** Train **XGB regressor** to predict noises in raw accelerometer data.
- **Implementation of the Modified CF:** Implementation of our proposed algorithm in python and evaluating it through the BROAD dataset trials.

## Testing: Dataset

---

- **Evaluation Setup:** Cross-validation set  $\{8, 14, 17, 22, 30\}$  used to estimate quaternions; error = mean quaternion distance between estimated and ground truth per recording.

## Testing: Dataset

---

- **Evaluation Setup:** Cross-validation set  $\{8, 14, 17, 22, 30\}$  used to estimate quaternions; error = mean quaternion distance between estimated and ground truth per recording.
- **Hyperparameter Selection:** Empirical tuning + grid search. Optimal values:  $\alpha = 0.001$ ,  $d_h = 120$ ,  $d_l = 60$  (balancing drift, responsiveness, smoothness).

## Testing: Dataset

---

- **Evaluation Setup:** Cross-validation set  $\{8, 14, 17, 22, 30\}$  used to estimate quaternions; error = mean quaternion distance between estimated and ground truth per recording.
- **Hyperparameter Selection:** Empirical tuning + grid search. Optimal values:  $\alpha = 0.001$ ,  $d_h = 120$ ,  $d_l = 60$  (balancing drift, responsiveness, smoothness).
- **Dataset Dependence:** Parameters may be overfitted to dataset noise/motion patterns; may not generalize to other datasets or devices with different sensor characteristics.

# Testing: Mechanical Turntable

---

- **Design & Construction:** Built in Fusion360, 3D-printed PLA/ABS parts, 28 cm diameter, 1.5 kg mass. Manual actuation (no motor); rotation applied by hand.

# Testing: Mechanical Turntable

---

- **Design & Construction:** Built in Fusion360, 3D-printed PLA/ABS parts, 28 cm diameter, 1.5 kg mass. Manual actuation (no motor); rotation applied by hand.
- **Mechanical Components:**
  - Circular rotating disk on 6010 bearing.
  - Box-shaped support structure with encoder magnet in base.
  - AS5600 magnetic encoder for ground-truth sensing.

# Testing: Mechanical Turntable

---

- **Design & Construction:** Built in Fusion360, 3D-printed PLA/ABS parts, 28 cm diameter, 1.5 kg mass. Manual actuation (no motor); rotation applied by hand.
- **Mechanical Components:**
  - Circular rotating disk on 6010 bearing.
  - Box-shaped support structure with encoder magnet in base.
  - AS5600 magnetic encoder for ground-truth sensing.
- **Ground-Truth Encoder (AS5600):** 12-bit resolution ( $\approx 0.087^\circ/\text{step}$ ),  $\pm 0.4^\circ$  typical accuracy, up to  $\pm 1.4^\circ$  deviation under misalignment. Latency: 1–2 ms, outputs via I2C, PWM, or analog.

# Testing: Mechanical Turntable

---

- **Design & Construction:** Built in Fusion360, 3D-printed PLA/ABS parts, 28 cm diameter, 1.5 kg mass. Manual actuation (no motor); rotation applied by hand.
- **Mechanical Components:**
  - Circular rotating disk on 6010 bearing.
  - Box-shaped support structure with encoder magnet in base.
  - AS5600 magnetic encoder for ground-truth sensing.
- **Ground-Truth Encoder (AS5600):** 12-bit resolution ( $\approx 0.087^\circ/\text{step}$ ),  $\pm 0.4^\circ$  typical accuracy, up to  $\pm 1.4^\circ$  deviation under misalignment. Latency: 1–2 ms, outputs via I2C, PWM, or analog.
- **On-Disk Payload:** Raspberry Pi 5 (8 GB), MPU9250 MARG sensor, 20,000 mAh power bank.

# Mechanical Turntable Setup

---

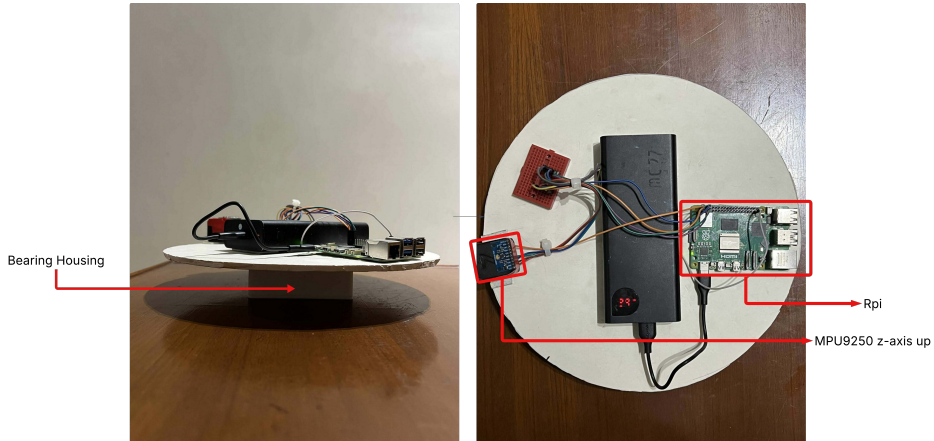


Figure: Mechanical Turntable side view (left) and top view (right).

# Motion Protocols & Software Setup

---

- **Motion Protocols:**
  - **Static:** No movement; tests sensor stability and drift.
  - **Quasi-static:** Slow  $0^\circ$ – $180^\circ$  rotation (clockwise & counterclockwise), two cycles per axis.
  - **Dynamic:** Continuous rapid rotations (3, 4, 5 turns per cycle).

# Motion Protocols & Software Setup

---

- **Motion Protocols:**
  - **Static:** No movement; tests sensor stability and drift.
  - **Quasi-static:** Slow  $0^\circ$ – $180^\circ$  rotation (clockwise & counterclockwise), two cycles per axis.
  - **Dynamic:** Continuous rapid rotations (3, 4, 5 turns per cycle).
- **Software Infrastructure:**
  - Raspberry Pi runs 4 parallel Python scripts: Proposed Filter, AQUA, EKF, Madgwick.
  - Reads MPU9250 sensor (accel, gyro, mag) via I2C.
  - AS5600 encoder provides ground-truth quaternions.
  - All filter outputs + ground truth logged into CSV for post-processing.

# Motion Protocols & Software Setup

---

- **Motion Protocols:**
  - **Static:** No movement; tests sensor stability and drift.
  - **Quasi-static:** Slow  $0^\circ$ – $180^\circ$  rotation (clockwise & counterclockwise), two cycles per axis.
  - **Dynamic:** Continuous rapid rotations (3, 4, 5 turns per cycle).
- **Software Infrastructure:**
  - Raspberry Pi runs 4 parallel Python scripts: Proposed Filter, AQUA, EKF, Madgwick.
  - Reads MPU9250 sensor (accel, gyro, mag) via I2C.
  - AS5600 encoder provides ground-truth quaternions.
  - All filter outputs + ground truth logged into CSV for post-processing.
- **Result Generation:** Quaternion absolute distance metric (Sec. 9.2) computed and plotted to compare filter performance under each motion type.

## **Satisfactory Results**

---

# Results of $\alpha$ -toggling with and without denoising across cross-validation files in BROAD

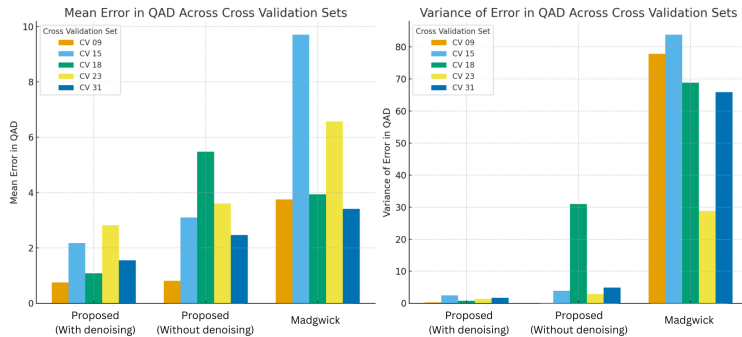


Figure: Mean error statistics (with and with denoising) across cross-validation files in BROAD

# Quasi-Static Error Metrics in Z-axis

Table: Quasi-Static error metrics ( $^{\circ}$ ) in Z-axis

Metric	Prop. (ML)	Prop. (no ML)	Madg.	Aqua	EKF
mean	9.84	<b>7.5</b>	7.98	10.08	32.2
std	10.33	<b>7.26</b>	9.77	18.77	18.122

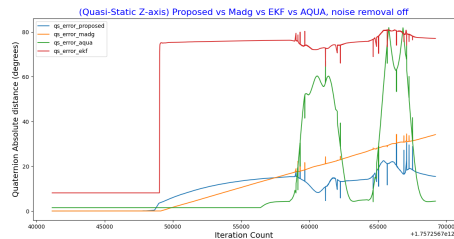
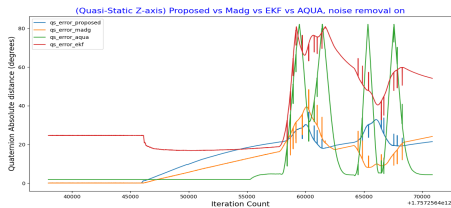


Figure: Quasi-Static Error with Denoising (Z-axis)

Figure: Quasi-Static Error without Denoising (Z-axis)

# Dynamic Error Metrics in X-axis

Table: Dynamic error metrics ( $^{\circ}$ ) in X-axis

Metric	Prop. (ML)	Prop. (no ML)	Madg.	Aqua	EKF
mean	30.87	<b>22.12</b>	32.35	24.36	47.57
std	31.33	<b>18.87</b>	31.86	31.06	19.17

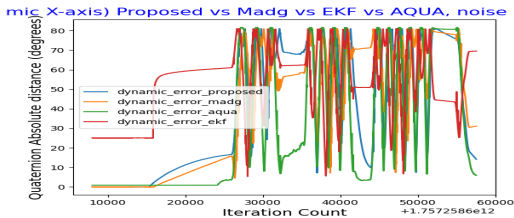


Figure: Dynamic Error with Denoising (X-axis)

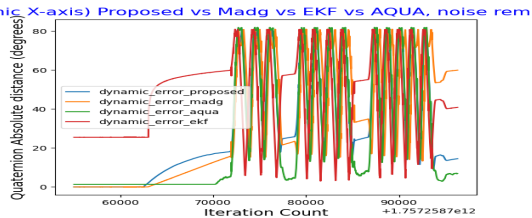


Figure: Dynamic Error without Denoising (X-axis)

# Dynamic Error Metrics in Z-axis

Table: Dynamic error metrics ( $^{\circ}$ ) in Z-axis

Metric	Prop. (ML)	Prop. (no ML)	Madg.	Aqua	EKF
mean	29.80	<b>10.14</b>	25.41	17.95	30.07
std	28.14	<b>11.72</b>	26.86	24.03	17.38

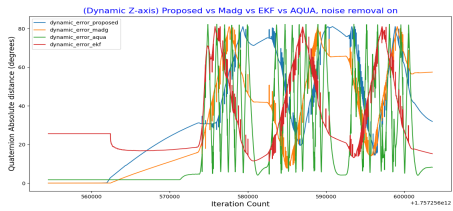


Figure: Dynamic Error with Denoising (Z-axis)

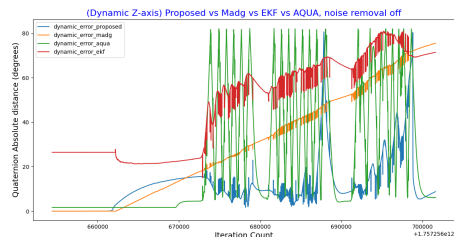


Figure: Dynamic Error without Denoising (Z-axis)

## **Unsatisfactory Results**

---

# Static Error Metrics with and without ML Denoising

Table: Static error metrics ( $^{\circ}$ ).

Metric	Prop. (ML)	Prop. (no ML)	Madg.	Aqua	EKF
mean	23.1	14.99	79.71	<b>10.64</b>	39.05
std	2.24	<b>1.06</b>	8.44	2.16	19.18

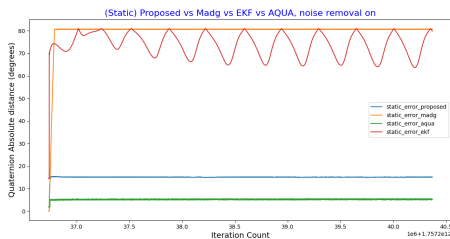


Figure: Static Error with Denoising

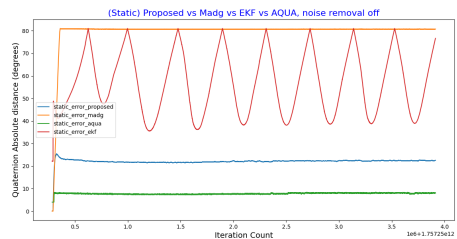


Figure: Static Error without Denoising

# Quasi-Static Error Metrics in X-axis

Table: Quasi-Static error metrics ( $^{\circ}$ ) in X-axis

Metric	Prop. (ML)	Prop. (no ML)	Madg.	Aqua	EKF
mean	16.25	14.06	13.45	<b>12.32</b>	52.278
std	22.04	<b>21.03</b>	21.15	23.9	15.32

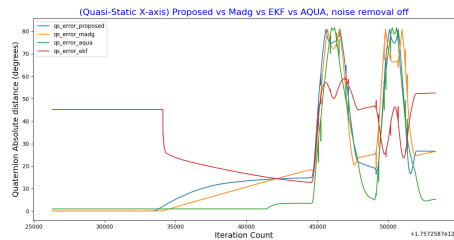
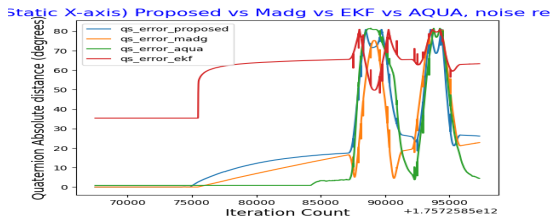


Figure: Quasi-Static Error with Denoising (X-axis)

Figure: Quasi-Static Error without Denoising (X-axis)

# Quasi-Static Error Metrics in Y-axis

Table: Quasi-Static error metrics ( $^{\circ}$ ) in Y-axis

Metric	Prop. (ML)	Prop. (no ML)	Madg.	Aqua	EKF
mean	18.04	17.36	14.77	<b>11.44</b>	40.89
std	23.01	24.10	23.89	23.92	<b>17.5</b>

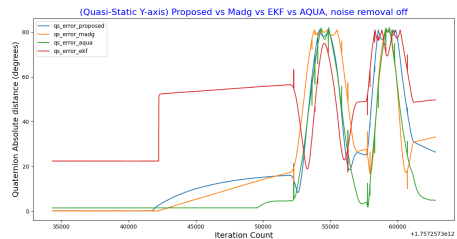
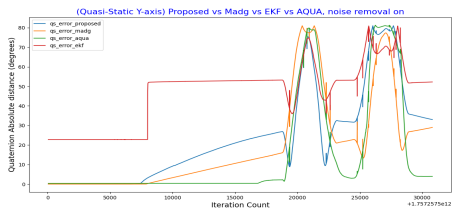


Figure: Quasi-Static Error with Denoising (Y-axis)

Figure: Quasi-Static Error without Denoising (Y-axis)

# Dynamic Error Metrics in Y-axis

Table: Dynamic error metrics ( $^{\circ}$ ) in Y-axis

Metric	Prop. (ML)	Prop. (no ML)	Madg.	Aqua	EKF
mean	26.92	33.97	29.90	<b>22.54</b>	44.08
std	28.90	29.95	30.74	28.58	<b>24.48</b>

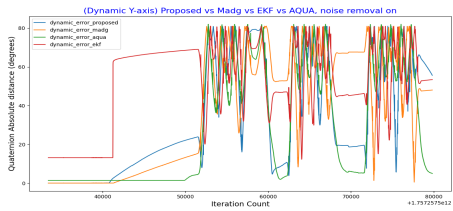


Figure: Dynamic Error with Denoising (Y-axis)

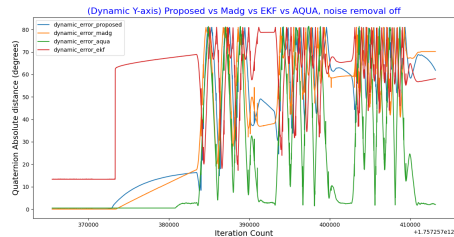


Figure: Dynamic Error without Denoising (Y-axis)

# Resource Consumption

---

Table: Static Error Resource consumption per filter on RPI: average CPU (%) and memory (MB).

Filter	CPU Usage (%)	Memory Usage (MB)
Proposed (ML)	58.6	145.65
Proposed (-ML)	54.5	120.35
Madgwick	<b>1.75</b>	59.75
EKF	3.12	59.77
Aqua	2.32	<b>59.69</b>

## **Shortcomings**

---

# Shortcomings of Our Data-Driven CF

---

- **Model Size & Memory:** XGBoost inference is  $O(\log n)$  per tree (depth=15, 6 vars, 15 estimators) → wide trees consume significant memory.

# Shortcomings of Our Data-Driven CF

---

- **Model Size & Memory:** XGBoost inference is  $O(\log n)$  per tree (depth=15, 6 vars, 15 estimators) → wide trees consume significant memory.
- **Computational Overhead:**
  - Matrix exponentiation for  $R_g$  rotations.
  - RANSAC-based training adds extra latency.

# Shortcomings of Our Data-Driven CF

---

- **Model Size & Memory:** XGBoost inference is  $O(\log n)$  per tree (depth=15, 6 vars, 15 estimators) → wide trees consume significant memory.
- **Computational Overhead:**
  - Matrix exponentiation for  $R_g$  rotations.
  - RANSAC-based training adds extra latency.
- **Training Time:** RANSAC loop and ensemble fitting are time-intensive.

# Shortcomings of Our Data-Driven CF

---

- **Model Size & Memory:** XGBoost inference is  $O(\log n)$  per tree (depth=15, 6 vars, 15 estimators) → wide trees consume significant memory.
- **Computational Overhead:**
  - Matrix exponentiation for  $R_g$  rotations.
  - RANSAC-based training adds extra latency.
- **Training Time:** RANSAC loop and ensemble fitting are time-intensive.
- **Generalizability:** Noticeable drop in performance on cross-validation vs. test sets.

# Shortcomings of Our Data-Driven CF

---

- **Model Size & Memory:** XGBoost inference is  $O(\log n)$  per tree (depth=15, 6 vars, 15 estimators) → wide trees consume significant memory.
- **Computational Overhead:**
  - Matrix exponentiation for  $R_g$  rotations.
  - RANSAC-based training adds extra latency.
- **Training Time:** RANSAC loop and ensemble fitting are time-intensive.
- **Generalizability:** Noticeable drop in performance on cross-validation vs. test sets.
- **Inconsistency in Axes:** Model seems to perform much better in z-axis but can't keep up the consistency in x and y axes.

## **Future Works**

---

# Future Works

---

- Improving generlizability

# Future Works

---

- Improving generlizability
- Improving the error statistics on x and y axes

# Future Works

---

- Improving generlizability
- Improving the error statistics on x and y axes
- Improving computational cost and memory usage

# Future Works

---

- Improving generlizability
- Improving the error statistics on x and y axes
- Improving computational cost and memory usage
- Studying the effect of using data-driven methods like ML denoising

# Deployment Challenges & Strategy

---

## Challenge: Resource Constraints

- XGBoost model size: 25MB flash memory

## Proposed Strategy

# Deployment Challenges & Strategy

---

## Challenge: Resource Constraints

- XGBoost model size: 25MB flash memory
- ESP32 max flash: 4MB

## Proposed Strategy

# Deployment Challenges & Strategy

---

## Challenge: Resource Constraints

- XGBoost model size: 25MB flash memory
- ESP32 max flash: 4MB
- Limited CPU and RAM on embedded platforms

## Proposed Strategy

# Deployment Challenges & Strategy

---

## Challenge: Resource Constraints

- XGBoost model size: 25MB flash memory
- ESP32 max flash: 4MB
- Limited CPU and RAM on embedded platforms

## Proposed Strategy

- **Model Optimization:**

# Deployment Challenges & Strategy

---

## Challenge: Resource Constraints

- XGBoost model size: 25MB flash memory
- ESP32 max flash: 4MB
- Limited CPU and RAM on embedded platforms

## Proposed Strategy

- **Model Optimization:**
  - Quantization & pruning

# Deployment Challenges & Strategy

---

## Challenge: Resource Constraints

- XGBoost model size: 25MB flash memory
- ESP32 max flash: 4MB
- Limited CPU and RAM on embedded platforms

## Proposed Strategy

- **Model Optimization:**
  - Quantization & pruning
  - Tree depth reduction

# Deployment Challenges & Strategy

---

## Challenge: Resource Constraints

- XGBoost model size: 25MB flash memory
- ESP32 max flash: 4MB
- Limited CPU and RAM on embedded platforms

## Proposed Strategy

- **Model Optimization:**
  - Quantization & pruning
  - Tree depth reduction
  - Converter to light-weight formats (e.g., Treelite)

# Deployment Challenges & Strategy

---

## Challenge: Resource Constraints

- XGBoost model size: 25MB flash memory
- ESP32 max flash: 4MB
- Limited CPU and RAM on embedded platforms

## Proposed Strategy

- **Model Optimization:**
  - Quantization & pruning
  - Tree depth reduction
  - Converter to light-weight formats (e.g., Treelite)
- **Fallback Deployment:**

# Deployment Challenges & Strategy

---

## Challenge: Resource Constraints

- XGBoost model size: 25MB flash memory
- ESP32 max flash: 4MB
- Limited CPU and RAM on embedded platforms

## Proposed Strategy

- **Model Optimization:**
  - Quantization & pruning
  - Tree depth reduction
  - Converter to light-weight formats (e.g., Treelite)
- **Fallback Deployment:**
  - If ESP32 still infeasible, deploy on Raspberry Pi

# Deployment Challenges & Strategy

---

## Challenge: Resource Constraints

- XGBoost model size: 25MB flash memory
- ESP32 max flash: 4MB
- Limited CPU and RAM on embedded platforms

## Proposed Strategy

- **Model Optimization:**
  - Quantization & pruning
  - Tree depth reduction
  - Converter to light-weight formats (e.g., Treelite)
- **Fallback Deployment:**
  - If ESP32 still infeasible, deploy on Raspberry Pi
  - Leverage its higher memory and CPU capabilities

## Sample bibliography (not shown in presentation, just for reference)

## References

---

# References I

---

- [1] “A robust complementary filter approach for attitude estimation of unmanned aerial vehicles using AHRS,” in *Proceedings of the 2019 CEAS EuroGNC conference*, CEAS-GNC-2019-036, Milan, Italy, Apr. 2019.
- [2] A. Asgharpoor Golroudbari and M. Sabour, *End-to-end deep learning framework for real-time inertial attitude estimation using 6dof imu*, Feb. 2023. DOI: [10.22541/au.167628608.89589390/v1](https://doi.org/10.22541/au.167628608.89589390/v1)
- [3] H. D. Black, “A passive system for determining the attitude of a satellite,” *AIAA journal*, vol. 2, no. 7, pp. 1350–1351, 1964.
- [4] M. Brossard, S. Bonnabel, and A. Barrau, “Denoising imu gyroscopes with deep learning for open-loop attitude estimation,” *IEEE Robotics and Automation Letters*, vol. 5, no. 3, pp. 4796–4803, 2020. DOI: [10.1109/LRA.2020.3003256](https://doi.org/10.1109/LRA.2020.3003256)

## References II

---

- [5] A. Cariow and G. Cariowa, "A hardware-efficient approach to computing the rotation matrix from a quaternion," *arXiv preprint arXiv:1609.01585*, 2016.
- [6] C. Chen and X. Pan, "Deep learning for inertial positioning: A survey," *IEEE Transactions on Intelligent Transportation Systems*, vol. 25, no. 9, pp. 10 506–10 523, 2024. DOI: 10.1109/TITS.2024.3381161
- [7] Y. Chen and H. Rong, "A customized extended kalman filter for removing the impact of the magnetometer's measurements on inclination determination," *Sensors*, vol. 23, no. 24, 2023, ISSN: 1424-8220. DOI: 10.3390/s23249756 [Online]. Available: <https://www.mdpi.com/1424-8220/23/24/9756>
- [8] R. K. R. Damagatla and M. Atia, "Improved imu/gnss ekf fusion using xgboost machine learning algorithm," in *2024 14th International Conference on Electrical Engineering (ICEENG)*, 2024, pp. 276–281. DOI: 10.1109/ICEENG58856.2024.10566377

## References III

---

- [9] M. B. Del Rosario, N. H. Lovell, and S. J. Redmond, "Quaternion-based complementary filter for attitude determination of a smartphone," *IEEE Sensors Journal*, vol. 16, no. 15, pp. 6008–6017, 2016. DOI: 10.1109/JSEN.2016.2574124
- [10] M. P. van Dijk, M. Kok, M. A. M. Berger, M. J. M. Hoozemans, and D. H. E. J. Veeger, "Machine learning to improve orientation estimation in sports situations challenging for inertial sensor use," *Frontiers in Sports and Active Living*, vol. Volume 3 - 2021, 2021, ISSN: 2624-9367. DOI: 10.3389/fspor.2021.670263 [Online]. Available: <https://www.frontiersin.org/journals/sports-and-active-living/articles/10.3389/fspor.2021.670263>
- [11] W. T. Higgins, "A comparison of complementary and kalman filtering," *IEEE Transactions on Aerospace and Electronic Systems*, vol. AES-11, no. 3, pp. 321–325, 1975. DOI: 10.1109/TAES.1975.308081

## References IV

---

- [12] D. Laidig, M. Caruso, A. Cereatti, and T. Seel, "Broad—a benchmark for robust inertial orientation estimation," *Data*, vol. 6, no. 7, p. 72, 2021.
- [13] S. O. Madgwick, A. J. Harrison, and R. Vaidyanathan, "Estimation of imu and marg orientation using a gradient descent algorithm," in *2011 IEEE international conference on rehabilitation robotics*, ieee, 2011, pp. 1–7.
- [14] R. Mahony, T. Hamel, and J.-M. Pflimlin, "Nonlinear complementary filters on the special orthogonal group," *IEEE Transactions on automatic control*, vol. 53, no. 5, pp. 1203–1218, 2008.
- [15] J. Marins, X. Yun, E. Bachmann, R. McGhee, and M. Zyda, "An extended kalman filter for quaternion-based orientation estimation using marg sensors," in *Proceedings 2001 IEEE/RSJ International Conference on Intelligent Robots and Systems. Expanding the Societal Role of Robotics in the the Next Millennium (Cat. No.01CH37180)*, vol. 4, 2001, 2003–2011 vol.4. DOI: 10.1109/IROS.2001.976367

## References V

---

- [16] A. Sabatini, "Quaternion-based extended kalman filter for determining orientation by inertial and magnetic sensing," *IEEE Transactions on Biomedical Engineering*, vol. 53, no. 7, pp. 1346–1356, 2006. DOI: 10.1109/TBME.2006.875664
- [17] W. Shao, J. Zang, J. Zhao, and K. Liu, "A variable gain complementary filtering fusion algorithm based on distributed inertial network and flush air data sensing," *Applied Sciences*, vol. 13, no. 14, 2023, ISSN: 2076-3417. DOI: 10.3390/app13148090 [Online]. Available: <https://www.mdpi.com/2076-3417/13/14/8090>
- [18] R. Valenti, I. Dryanovski, and J. Xiao, "Keeping a good attitude: A quaternion-based orientation filter for imus and margs," *Sensors*, vol. 15, pp. 19 302–19 330, Aug. 2015. DOI: 10.3390/s150819302

## References VI

---

- [19] E. Vertzberger and I. Klein, "Adaptive attitude estimation using a hybrid model-learning approach," *IEEE Transactions on Instrumentation and Measurement*, vol. 71, pp. 1–9, 2022.
- [20] S. Zhao, "Time derivative of rotation matrices: A tutorial," *arXiv preprint arXiv:1609.06088*, 2016.

**Thank you!**